Helmholtz-Zentrum
Geesthacht
Zentrum für Material- und Küstenforschung

# *Final Draft*
## of the original manuscript:

Mazurek-Budzynska, M.; Razzaq, M.Y.; Tomczyk, K.; Rokicki, G.; Behl, M.; Lendlein, A.:
**Poly(carbonate-urea-urethane) networks exhibiting high-strain shape-memory effect.**
In: Polymers for Advanced Technologies. Vol. 28 (2017) 10, 1285 - 1293.
First published online by Wiley: 24.10.2016

http://dx.doi.org/10.1002/pat.3948

# Poly(carbonate-urea-urethane) networks exhibiting high-strain shape-memory effect

Magdalena Mazurek-Budzyńska [1,2,*], Muhammad Yasar Razzaq [1], Karolina Tomczyk [2], Gabriel Rokicki [2], Marc Behl [1] and Andreas Lendlein [1]

[1] *Institute of Biomaterial Science, Helmholtz-Zentrum Geesthacht, Kantstr. 55, 14513 Teltow, Germany*

[2] *Warsaw University of Technology, Department of Chemistry, ul. Noakowskiego 3, 00-664 Warsaw, Poland*

* *Corresponding author: magdalena.mazurek-budzynska@hzg.de*

**Abstract**

A challenge in the design of shape-memory polymers (SMPs) is to achieve high deformability with a simultaneous high shape recovery ratio. Here we explored, whether SMPs featuring large deformation capability and high shape recovery ratios can be created as polymer networks providing two kinds of netpoints based on covalent bonds and physical interactions. As a model system we selected poly(carbonate-urea-urethane)s (PCUUs) synthesized by a precursor route, based on oligo(alkylene carbonate) diols, isophorone diisocyanate (IPDI), and water vapor. The PCUU networks exhibited an one-way shape-memory effect (1W-SME) with programmed strains up to $\varepsilon_{prog}$ = 1000% whereby they provided excellent shape fixity (92-97%) and shape recovery (≥ 99%) ratios. The switching temperatures ($T_{sw}$) varied between 36 and 65 °C and increased with the increasing molecular weight of the oligo(alkylene carbonate) diol and length of the hydrocarbon chain between the carbonate linkages. $T_{sw}$ was also influenced by the strain applied during programming ($\varepsilon_{prog}$). Poly(carbonate-urethane)s have been reported to have good biocompatibility and biostability, which in the combination of high-strain capacity and high Young's modulus makes the obtained PCUUs interesting candidate materials suitable for medical devices such as medical sutures or vascular stents.

**Keywords:** Poly(carbonate-urea-urethane)s, oligo(alkylene carbonate) diols, one-way high-strain shape-memory effect.

## Introduction

Thermoplastic shape-memory polyurethanes (SMPURs) with tunable thermal and mechanical properties have been widely investigated as they are well suited for a broad variety of processing methods.[1-3] SMPUR are characterized by a phase-segregated structure, in which the switching domains act as temporary netpoints, and hard domains determine the permanent shape. SMPURs provide a high deformability but exhibit low shape recovery. The recovery behavior strongly relates to the degree of crystallization, stress relaxation, and creep.[4,5] Due to these factors, to achieve a high shape recovery ratio ($R_r > 90\%$), the programming strain of thermoplastic polymers typically do not exceed 400%.[4,6] In contrast, shape-memory polymers (SMPs) based on covalent networks have shown high shape recovery ratios but exhibit a limited elastic deformation capacity.[2,7-10] Furthermore, many applications for biomedical devices require large shape changes as the devices need to be inserted through small incisions or in a minimally-invasive way by the usage of catheters, and subsequently need to recover their original, application relevant shape. Thus far, only a few examples of covalently crosslinked SMP with high recoverable strains have been reported. Recoverable strains of 800% and a shape fixity ratio $R_f \approx 99\%$ were obtained in copolymer systems based on methyl acrylate and isobornyl acrylate crosslinked by bisphenol A ethoxylate di(meth)acrylate.[6] SMP networks containing ε-caprolactone (PCL) as a switching segment, 4,4'-methylenediphenyl diisocyanate, and surface modified $SiO_2$ microspheres as netpoints have been reported to achieve $R_f \approx 100\%$ and $R_r \approx 99\%$, when a programming strain of 500% was applied.[11] Recently, methyl acrylate and methyl methacrylate copolymer networks with movable netpoints of an interlocked slide-ring structure were reported to have $R_f = 94$ % and $R_r = 92$ % after 800% of deformation.[12]

The aim of this work was to create a SMP network, which would have an even higher deformability compared to already reported shape-memory polymer networks and simultaneously a high shape recovery ratio. We hypothesized that these intended properties of SMPs could be realized by creating a polymer network providing two kinds of netpoints – covalent bonds and physical interactions. As a model system we selected poly(carbonate-urea-urethane)s (PCUUs) synthesized by a precursor route. To achieve high fixation of a temporary shape we selected highly crystallisable precursors, which are intended to form temporary netpoints: oligo(alkylene carbonate) diols (OCDs) with long hydrocarbon chains between carbonate linkages. We expected that various morphologies of OCDs would result in different mechanical and thermal properties as

well as the shape-memory behavior of PCUUs. Furthermore, OCDs have been reported to improve the biostability of polyurethanes (PURs) when compared to those based on polyesters and polyethers, which is essential for purposes of long-term medical applications, we would like to achieve by our PCUU system.[13-21]

In the first step the oligo(alkylene carbonate) diols were functionalized with an excess of diisocyanate to obtain diisocyanate telechelics. Afterwards, a moisture-curing process,[22,23] in which water vapors were added to hydrolyze the isocyanate to amine groups, was applied. The reaction of the amine with diisocyanate groups, which is much faster than the hydrolysis of the isocyanate groups, resulted in polymer chain extension whereby urea groups were formed. These urea groups contribute to the physical interactions among the hard segment domains. In addition, small amounts of covalent bonds acting as permanent netpoints were created by using an excess of the diisocyanate monomer. It was confirmed in one of the previous studies,[23] that inter-molecular covalent bonds based on allophanate and biuret groups formation can occur even when the synthesis is performed at T ≤ 80 °C and without usage of a catalyst. However, the contribution of those crosslinks was very low and did not exceed 8%.[23] Limited amounts of permanent netpoints were expected to enable high deformation capability of the PCUU networks.

Systematic studies of PCUUs were performed to analyze the relationship between the structure and morphology of the obtained PCUU networks and the shape-memory properties. Here in particular we explored the influence of the switching segment molecular weight, distance between the carbonate linkages, as well as the programmed deformation ($\varepsilon_{prog}$) on switching temperature ($T_{sw}$), shape fixity ($R_f$), and shape recovery ($R_r$) ratios. The microstructural changes in crystalline phase during the shape-memory experiments were studied by wide angle X-ray scattering (WAXS).

## Experimental

### 1.1. Materials

Chloroform (purity ≥ 99.9%), hydrochloric acid (purity ≥ 99.9%) (POCH, Gliwice, Poland), *d*-Chloroform ($CDCl_3$) (purity ≥ 99%), 1,10-decanediol (purity 98%), dimethyl carbonate (DMC) (purity 99%), 1,12-dodecanediol (purity ≥ 98.0%), isophorone diisocyanate (IPDI) (purity 98%), 1,9-nonanediol (purity 98%), titanium(IV) butoxide (purity ≥ 97%) (Sigma-Aldrich, Poznan, Poland) were used as received.

### 1.2. Characterization techniques

$^1$H NMR spectra of oligo(alkylene carbonate) diols (OCDs) were recorded at room temperature on a Varian VXR 400 MHz spectrometer using tetramethylsilane as an internal reference and $CDCl_3$ as solvent, and were analyzed with MestReNovav.6.2.0-7238 (Mestrelab Research S.L) software.

Densities of samples were determined with an Ultra Pycnometer (Quantachrome, Odelzhausen, Germany) at 25 °C using a measurement cell with a calibration volume of 1.0725 $cm^3$.

Wide angle X-ray scattering (WAXS) measurements were conducted on a D8 Discover X-ray diffractometer from Bruker AXS (Karlsruhe, Germany) in transmission geometry (X-ray generator operated at 40 kV and 40 mA) with a two-dimensional Hi-Star detector (Bruker AXS, Karlsruhe, Germany). The X-ray beam (Cu Kα-radiation, λ = 0.154 nm) was provided by a graphite monochromator and a pinhole collimator with an opening of 0.8 mm. Sample-to-detector distance was 15 cm. Exposure time of 120 s per scattering pattern was applied. An integration over an angle chi χ = 120° and the whole 2$\theta$-range was performed to obtain 1D-scattering curves using 5-point normalized binning. In case of deformed (oriented) samples integration over the strongest reflection (in radial angle chi χ) was performed to estimate the degree of orientation (*B*). The scattering curves of semi-crystalline samples were analysed with the Bruker-software Diffrac$^{plus}$ TOPAS 3.0. Peaks of amorphous and crystalline phases were fitted with Pearson VII functions. The relationship of the integrated areas determines the degree of crystallinity ($\chi_c$) (eq. 1).[24] Peak position and breadth (*B*) correlate to the crystal size ($l_c$) according to the Scherrer equation (eq. 2) (parameter k = 0.9)[25]

$$\chi_c = \frac{A_{cryst}}{A_{cryst}+A_{amorph}} \cdot 100\% \qquad (1)$$

$$l_c = \frac{k \cdot \lambda}{B \cdot cos\theta} \qquad (2)$$

where *B* is a full width at half maximum of the crystalline reflection (in radians), $\theta$ is a half scattering angle, $\lambda$ is the wavelength of X-rays (0.15418 nm).

Dynamic mechanical thermal analyses (DMTA) at varied temperatures were conducted with a Gabo (Ahlden, Germany) Eplexor 25 N. All experiments were performed in temperature sweep mode with a constant heating rate of 2 K·min$^{-1}$ and an oscillation frequency of 10 Hz. Samples were investigated in a temperature interval from -100 to 200 °C. Results of the measurements were

used to determine the crosslinking density ($\nu$) and the number average molecular weight of the polymer chain segments between the netpoints ($M_c$) based on storage modulus ($E'$) according to the eq. 3 and 4:

$$E' = \frac{3\rho\, RT}{M_c}, \qquad \nu = \frac{E'}{3\, RT} \qquad (3), (4)$$

Where $E'$ is the storage modulus, $\rho$ is the density of the sample, R is the gas constant and $T$ is the temperature (K). E' values at 70 °C (above melting transitions of the samples) were used for calculating $M_c$ and $\nu$.

Differential Scanning Calorimetry (DSC) measurements were performed on a DSC 204 Phoenix (Netzsch, Selb, Germany) with a constant heating and cooling rate of 10 $K \cdot min^{-1}$. Whenever the maximum or minimum temperature in the testing program was reached, the temperature was kept constant for 2 min. Samples of PCUU were investigated in a temperature range from -100 to 250 °C in three cycles: heating from 20 to 250 °C, then cooling to -100 °C and again heating to 250 °C. Measurements of oligo(alkylene carbonate) diols were performed in 3 cycles in the range of -100 to 100 °C. The melting ($T_m$) and glass transition ($T_g$) temperatures were determined from the second heating cycle, and the crystallization temperature ($T_c$) was determined from the cooling run.

The gel fraction content ($G_F$), the mass equilibrium degrees of swelling ($Q_m$), and the volumetric swelling ratio ($Q_v$) were determined by swelling the films in 100-fold excess (related to the sample weight) of chloroform for 72 hours at room temperature and subsequent drying at room temperature overnight. Endpoints of swelling and drying were reached when constant weights were obtained. The $G_F$ values were calculated as the ratio of the weights of the non-swollen ($m_d$), and the extracted ($m_{ex}$) sample according to equation 5.[26]

$$G_F = \frac{m_{ex}}{m_d} \qquad (5)$$

The mass equilibrium degrees of swelling ($Q_m$) were estimated by comparing initial weights of samples ($m_d$) and in the swollen state ($m_{sw}$) according to equation 6.[27]

$$Q_m = \frac{m_{sw} - m_d}{m_d} \qquad (6)$$

The volumetric degrees of swelling ($Q_v$) were estimated according to equation 7[26]

$$Q_v = 1 + \rho_2 \left(\frac{m_{sw}}{m_d \cdot \rho_1} - \frac{1}{\rho_1}\right) \qquad (7)$$

where $\rho_2$ is the density of dry polymer, $m_{sw}$ is the weight of polymer sample in the swollen state, $m_d$ is the weight of a dry polymer sample, $\rho_1$ is the density of a swelling medium (chloroform: $\rho_1 = 1.48$ g·cm$^{-3}$).

Cyclic, thermomechanical tests and tensile tests were conducted with standard samples (ISO 527-2/1BB) cut from films on a tensile tester Z75 (Zwick, Ulm, Germany) equipped with thermo-chamber (Zwick, Ulm, Germany), temperature controller Eurotherm control 2408 (Eurotherm Regler, Limburg, Germany) and load cells suitable to determine maximum forces of 200 N. The strain rate in uniaxial tensile test was 20 mm·min$^{-1}$ and in cyclic, thermomechanical test 5 mm·min$^{-1}$.

*Description of cyclic, thermomechanical tensile tests for one way shape-memory effect (1W-SME) investigation.*

The sample of PCUU was deformed to $\varepsilon_{prog}$ at $T_{prog}$. After keeping this deformation for 10 min to allow relaxation, the stress was held constant while the sample was cooled to $T_{low}$ with a cooling rate of 5 K·min$^{-1}$ whereby the sample elongated to $\varepsilon_l$. After unloading the stress ($\sigma_0$ = 30mN), the temporary shape $\varepsilon_u$ was fixed. Then the sample was heated to $T_{prog}$ with a heating rate of 5 K·min$^{-1}$, kept at this temperature for 10 min resulting in shape recovery to $\varepsilon_p$. Afterwards the next cycle was performed. The shape fixity ratio $R_f$ was calculated according to the eq. 8, and the ability of the material to recover its original shape was quantified by the shape recovery ratio $R_r$ (eq. 9).[28] $T_{sw}$ was determined at the inflection point of the elongation/temperature curve at the maximum of the absolute value of $\Delta\varepsilon/\Delta T$. Based on DSC thermograms values of $T_{prog}$ and $T_{low}$ were chosen and were 70 °C and 10 °C in case of PCUUs based on oligo(dodecamethylene carbonate), 60 °C and 0 °C in case of PCUUs based on oligo(decamethylene carbonate), and 50 °C and -10 °C in case of PCUUs based on oligo(nonamethylene carbonate) diols, respectively. $\varepsilon_{prog}$ has varied between 100 and 1000% and was limited by the maximum deformability achievable in the tensile tester.

$$R_f = \frac{\varepsilon_u(N)}{\varepsilon_l} \cdot 100\% \qquad (8)$$

$$R_r = \frac{\varepsilon_u(N) - \varepsilon_p(N)}{\varepsilon_u(N) - \varepsilon_p(N-1)} \cdot 100\% \qquad (9)$$

## 1.3. Syntheses

### 1.3.1. Synthesis of the oligo(alkylene carbonate) diols (OCDs)

OCDs were synthesized following the two-step condensation procedure reported in reference.[23] The alkylene bis(methylcarbonate)s (BMC) were prepared by reacting a high molar excess of dimethyl carbonate with the α,ω-diol (1,9-nona-, 1,10-deca-, 1,12-dodecanediol), in the presence of $Ti(OBu)_4$ as a catalyst. Afterwards OCDs of intended number average molecular weights ($M_n$s) were obtained by reacting the BMC with an appropriate molar excess of the α,ω-diol. To remove the catalyst from the OCDs, products were dissolved in chloroform and washed with a 3% aq. solution of HCl, followed by washing with distilled water and drying for 24h at 100 °C under reduced pressure. $M_n$s of OCDs were calculated based on the $^1$H NMR spectra. OCDs were named **OCD-9_X**, **OCD-10_Y,** and **OCD-12_Z**, where the number after the OCD represents the α,ω-diol (nona-, deca- and dodecanediol), and the following **X, Y** and **Z** indicate the $M_n$ of OCD.

### 1.3.2. Synthesis of poly(carbonate-urea-urethane) networks (PCUUs)

PCUU networks were synthesized following the precursor route, in which diisocyanate telechelics were obtained by reacting the different oligo(alkylene carbonate) diols with an excess of isophorone diisocyanate (IPDI). The subsequent curing process was performed in a climate chamber under controlled conditions of humidity and temperature. The procedure is described in details in our previous report.[23]

## 2. Results and discussion

### 2.1. Synthesis of oligo(alkylene carbonate) diols

Oligo(alkylene carbonate) diols with a $M_n$ in the range from 3000 to 5100 g·mol$^{-1}$ were obtained in a two-step polycondensation method.[23] In calorimetric measurements (DSC) no $T_g$ of OCDs could be recorded. A similar behaviour of carbonate oligomers with long hydrocarbon chains (above 8 methylene groups) was already reported, and explained by a very fast crystallization process.[29,30] Furthermore, with increasing number of methylene groups between the carbonate linkages, $T_m$ increased from 53 to 69 °C in case of **OCD-9_3000** and **OCD-12_3500**, respectively. However, no change of $T_m$ for **OCD-10s** with various $M_n$ was observed (Table 1).

**Table 1**. Thermal properties of obtained oligo(alkylene carbonate) diols.

| Sample | $T_m$ (°C) | $\Delta H_m$ (J·g$^{-1}$) | $T_c$ (°C) | $\Delta H_c$ (J·g$^{-1}$) |
|---|---|---|---|---|
| **OCD-9_3000** [a] | 53 ± 1 | 104 ± 1 | 31 ± 1 | 97 ± 1 |
| **OCD-10_3400** [b] | 59 ± 1 | 103 ± 1 | 39 ± 1 | 94 ± 1 |
| **OCD-10_5100** | 59 ± 1 | 100 ± 1 | 41 ± 1 | 89 ± 1 |
| **OCD-12_3500** [c] | 69 ± 1 | 120 ± 1 | 51 ± 1 | 111 ± 1 |

[a] **OCD-9_3000** - oligo(nonamethylene carbonate) diol with $M_n$ = 3,000 g·mol$^{-1}$.
[b] **OCD-10_3400** - oligo(decamethylene carbonate) diol with $M_n$ = 3,400 g·mol$^{-1}$.
[c] **OCD-12_3500** - oligo(dodecamethylene carbonate) diol with $M_n$ = 3,500 g·mol$^{-1}$.

### 2.2. Synthesis of PCUUs

The isocyanate telechelics were created by reacting OCDs (Table 1) with IPDI (Scheme 1). The synthesis was carried out without using a catalyst and solvent. A 3-molar excess of IPDI in relation to OCD was applied to enable cross-linking in the subsequent reaction step.

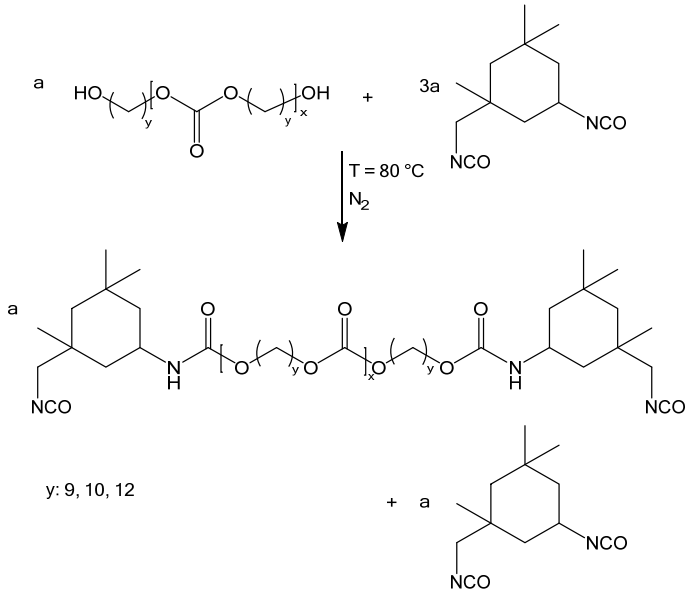


**Scheme 1**. Synthesis of isocyanate telechelics based on oligo(alkylene carbonate) diol and IPDI.

The chain extension reaction was performed under controlled conditions of humidity (5-40%) and temperature (60-75 °C). Water vapors were used to hydrolyze the isocyanate to amine groups. Following reaction of the amine with diisocyanate groups, which is much faster than hydrolysis of isocyanate groups, resulted in polymer chain extension whereby urea groups were formed (Scheme 2).[31]

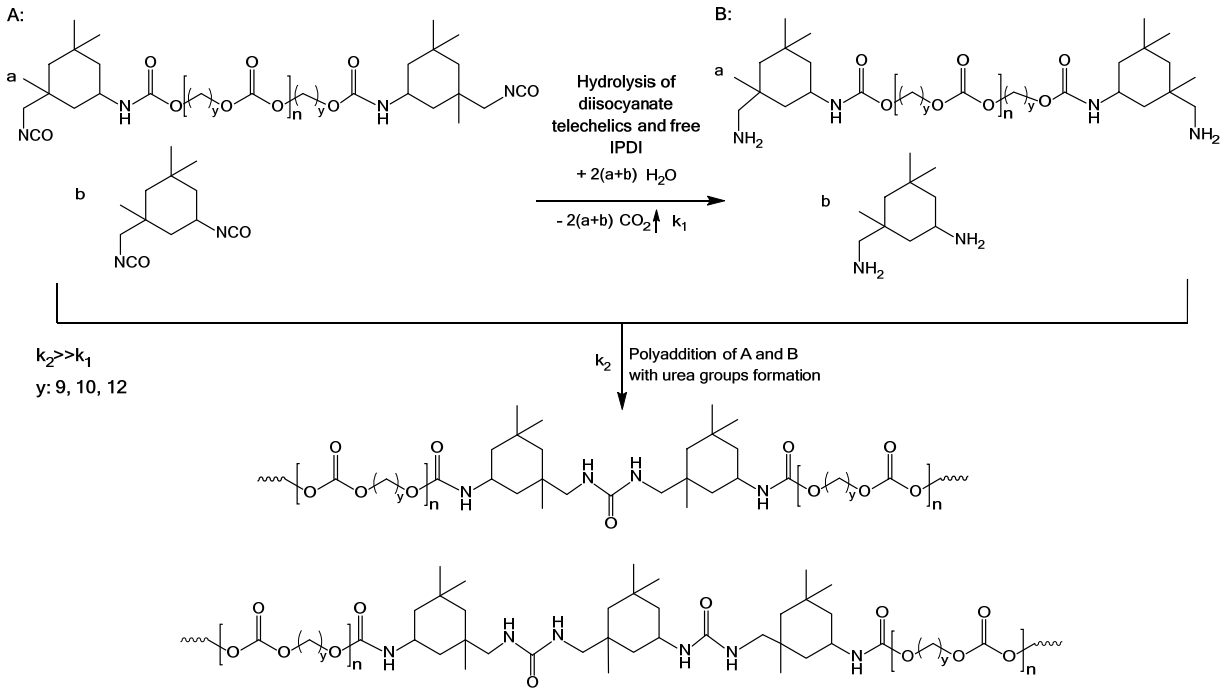


**Scheme 2**. Chain extending of the diisocyanate prepolymers.

The high excess of IPDI enabled the formation of a partially covalently crosslinked structure. By reaction of the isocyanate groups with urethane and urea groups, inter-molecular allophanate and biuret linkages were formed (Scheme 3). According to the chosen method, in which the applied temperature was below 80 °C and no catalyst was used, only a small amount of permanent netpoints based on allophanate and biuret linkages were expected.[23] The obtained products were insoluble in any of commonly available solvents because of covalent crosslinking bonds as well as the strong inter-molecular physical interactions based on hydrogen bonds.

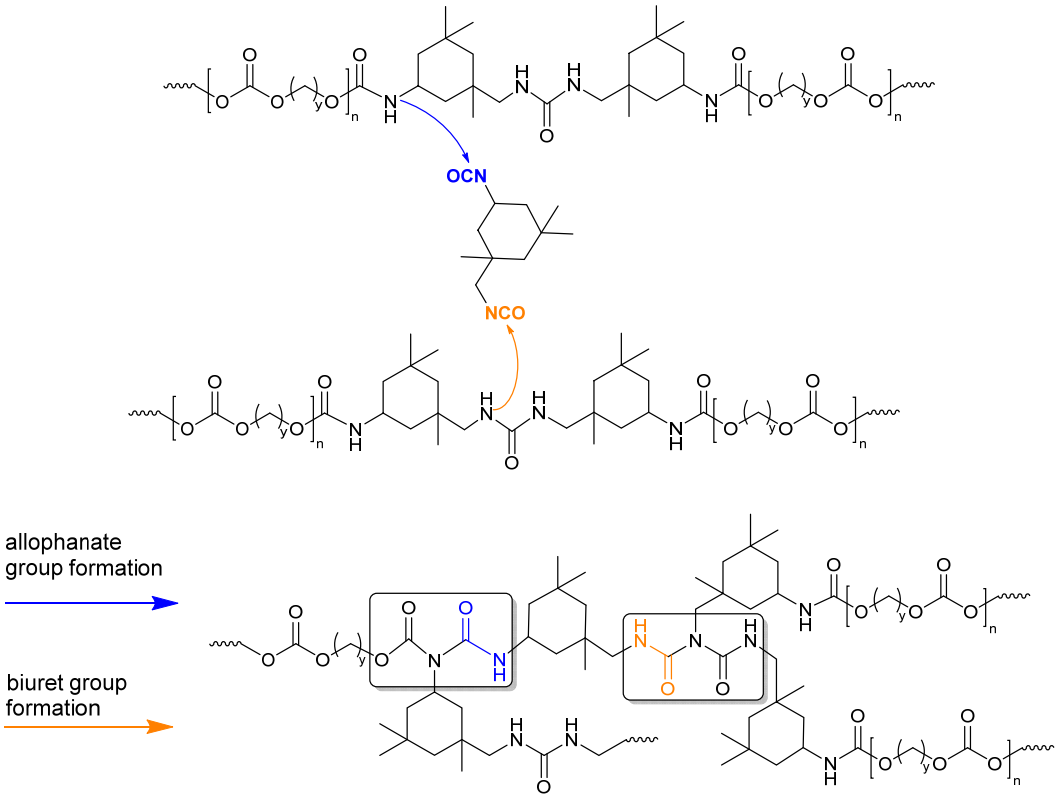


**Scheme 3**. Formation of inter-molecule allophanate and biuret bonds.

### 2.3. Materials structure and properties

There are several methods which can be used to determine the crosslinking densities of crosslinked polymers. Solvent swelling data can give absolute values for crosslinking density, however, it can only be obtained when accurate values of the Flory-Huggins polymer-solvent interaction parameter are available. Therefore, the crosslinking density ($\nu$) and the number average molecular weight between the netpoints ($M_c$) were estimated based on the value of the storage modulus in the rubbery plateau region obtained during the DMTA measurements (see Experimental section). With the increasing $M_n$ of the switching segment, the distance between hard segment domains increased, leading to a decrease of $\nu$ and to an increase of $M_c$ (Tab. 2). This relation was confirmed by the $G_F$, which was strongly decreasing with an increase of the switching segments' $M_n$. In addition, the values of $Q_v$ and $Q_m$ significantly increased with the increase of $M_n$ of the OCDs used as a switching segment.

**Table 2.** Swelling behavior and crosslinking densities of PCUUs.

| Sample | $\rho$ ($g \cdot cm^{-3}$) | $M_c$ [a] ($g \cdot mol^{-1}$) | $\nu$ [b] ($10^{-4} \cdot mol \cdot cm^{-3}$) | $G_F$ [c] (%) | $Q_m$ [d] (%) | $Q_v$ [e] (%) |
|---|---|---|---|---|---|---|
| **PCUU-9_3000** | 0.9937 ± 0.0067 | 1380 ± 70 | 7.6 ± 0.4 | 94 ± 2 | 1600 ± 75 | 1170 ± 50 |
| **PCUU-10_3400** | 1.0051 ± 0.0056 | 1440 ± 70 | 7.0 ± 0.3 | 95 ± 3 | 1550 ± 80 | 1150 ± 50 |
| **PCUU-10_5100** | 0.9729 ± 0.0053 | 1820 ± 90 | 5.0 ± 0.2 | 40 ± 2 | 6950 ± 10 | 4640 ± 10 |
| **PCUU-12_3500** | 1.0134 ± 0.0051 | 1700 ± 85 | 6.0 ± 0.3 | 83 ± 3 | 2860 ± 42 | 2050 ± 35 |

[a] $M_c$ - a number average molecular weight of polymer segments between two crosslinks determined by DMTA.
[b] $\nu$ - crosslinking density determined by DMTA.
[c] $G_F$ - gel fraction content in chloroform.
[d] $Q_m$ - mass equilibrium swelling ratio in chloroform.
[e] $Q_v$ - volumetric swelling ratio in chloroform.

$T_g$, $T_m$, and $T_c$ as well as the corresponding enthalpies ($\Delta H_m$, $\Delta H_c$) of the PCUUs' soft phase were determined by DSC analysis (Tab. 3). Exemplary graphs are shown for **PCUU-9_3000**, **PCUU-10_3400**, and **PCUU-12_3500** in Fig. 1. The ability of switching domains to crystallize increased with the increasing length of the hydrocarbon chain. This results in a higher stiffness of PCUU and in consequence higher value of $T_g$.

The WAXS measurements showed an increase of the degree of crystallinity ($\chi_c$) with increasing distance between carbonate linkages, as well as with increasing $M_n$ of the switching segment (Tab. 3). With higher $M_n$ of the switching segment, the distance between the hard and switching segment increases, which in consequence increases the ability to crystallize in the switching domains and results in higher phase separation. Similar relation between the degree of crystallinity and the molecular weight of the switching segment was observed in poly(carbonate-urethane)s.[29,32] The molecular weight of the oligocarbonate diols was 2000 $g \cdot mol^{-1}$, which was too low to observe high phase separation between the switching and hard domains of the polymer network. The critical molecular weight of around 2000-3000 $g \cdot mol^{-1}$, which has to be reached to obtain a crystalline phase formation within the switching domains, was also reported in PCL based polyurethanes.[33] For $M_{n,PCL}$ of 1600 and 2000 $g \cdot mol^{-1}$, no crystalline phase was detected, whereas for samples with $M_{n,PCL}$ of 4000 and 7000 $g \cdot mol^{-1}$, degree of crystallinity of around 30% was observed.

**Table 3.** Thermal and morphological properties of PCUUs based on DSC and WAXS measurement.

| Sample | $T_g$ (°C) | $T_m$ (°C) | $\Delta H_m$ (J·g$^{-1}$) | $T_c$ (°C) | $\Delta H_c$ (J·g$^{-1}$) | $l_c$ [a] (nm) | $\chi_c$ [b] (%) |
|---|---|---|---|---|---|---|---|
| **PCUU-9_3000** | -41 ± 1 | 37 ± 1 | 31 ± 1 | -18 ± 1 | 24 ± 1 | 14 ± 0.2 | 14 ± 0.2 |
| **PCUU-10_3400** | -33 ± 1 | 46 ± 1 | 41 ± 1 | 12 ± 1 | 41 ± 1 | 12 ± 0.2 | 18 ± 0.3 |
| **PCUU-10_5100** | -36 ± 1 | 43 ± 1 | 47 ± 1 | 22 ± 1 | 51 ± 1 | 13 ± 0.2 | 24 ± 2.2 |
| **PCUU-12_3500** | -27 ± 1 | 54 ± 1 | 39 ± 1 | 18 ± 1 | 45 ± 1 | 12 ± 0.2 | 22 ± 1.9 |

[a] $l_c$ – crystal size determined by WAXS.
[b] $\chi_c$ – degree of crystallinity determined by WAXS.

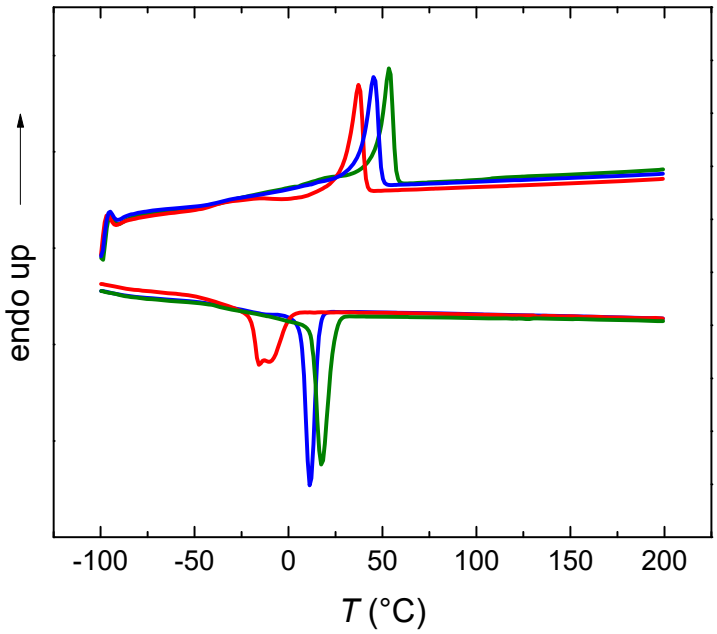


**Figure 1.** Thermograms of **PCUU-9_3000** (▬), **PCUU-10_3400** (▬) and **PCUU-12_3500** (▬) determined by DSC (10 Kmin$^{-1}$).

Uniaxial tensile tests were performed at room temperature (RT) and at $T > T_m$ to examine the deformation capability of the samples. At RT, with an increase of $M_n$ of the switching segments, values of maximum tensile strength ($\sigma_m$) decreased while simultaneously the maximum of elongation ($\varepsilon_m$) increased (Tab. 4). This behavior is strongly related to $v$, which decreases with an increase of $M_n$ of the switching segment as well as to the $\chi_c$, which increases with increasing $M_n$ of OCD (Tab. 2). An increase in distance between the carbonate linkages in the macromolecule leads to an increase of $\sigma_m$, the Young's moduli ($E$), as well as $\varepsilon_m$ (Tab. 4). This can be explained by an

increase of the $\chi_c$ as well as of the crosslinking density of PCUUs with increasing number of $CH_2$ groups between the carbonate linkages (Tab. 1). Above $T_m$ of the crystallisable switching segment (70 °C) a significant decrease of $E$ from 30-50 MPa to 3-4 MPa, as well as of $\sigma_m$ from 40-50 MPa to 9-11 MPa were observed, indicating a correlation between the thermal transition of the switching domains and the mechanical strength of the polymer. In addition, $\varepsilon_m$ was significantly higher at 70 °C as compared to the value at RT.

**Table 4.** Mechanical properties of PCUUs determined by tensile strength testing at RT and 70 °C.

| Sample | RT | | | 70 °C | | |
|---|---|---|---|---|---|---|
| | $E$ (MPa) | $\sigma_m$ (MPa) | $\varepsilon_m$ (%) | $E$ (MPa) | $\sigma_m$ (MPa) | $\varepsilon_m$ (%) |
| **PCUU-9_3000** | 17.5 ± 5.5 | 39.0 ± 2.0 | 810 ± 20 | 3.7 ± 0.1 | 11.0 ± 0.5 | 1025 ± 50 |
| **PCUU-10_3400** | 37.0 ± 4.5 | 42.5 ± 3.5 | 855 ± 35 | 2.5 ± 0.1 | 9.5 ± 2.0 | 1280 ± 95 |
| **PCUU-10_5100** | 40.0 ± 4.5 | 37.0 ± 3.5 | 900 ± 35 | 2.8 ± 0.2 | 10.5 ± 0.5 | 1220 ± 20 |
| **PCUU-12_3500** | 53.5 ± 9.5 | 43.0 ± 3.0 | 870 ± 15 | 2.9 ± 0.0 | 11.5 ± 2.0 | 1200 ± 90 |

### 2.4. Shape-memory properties

The concept of high deformation capability with simultaneous high recovery ratio was investigated by cyclic, thermomechanical tensile tests (see Experimental part).[8] Fixation of the temporary shape of the sample was performed in the stress-controlled conditions to achieve high shape fixity. Compared to programming under strain-controlled conditions, the stress-controlled programming results in a higher degree of chain orientation causing crystallization-induced elongation and in this way an increase of $\chi_c$. The influence of the programmed strain ($\varepsilon_{prog}$) as well the structure of the switching segment of PCUU on the shape-memory properties was investigated by cyclic, thermomechanical tensile tests, as well as DSC and WAXS analyses. Here, each cycle of thermomechanical tensile tests consists of heating the sample to $T_{prog}$ followed by elongation to $\varepsilon_{prog}$, then fixing the temporary shape by cooling the sample to $T_{low}$ with simultaneous release of the stress, and finally recovering the permanent shape of the sample under stress-free conditions by heating to $T_{prog}$. The macroscopic changes of the strain of the sample during cyclic, thermomechanical SME measurement are shown in Figure 2 exemplarily for **PCUU-10_5100** with $\varepsilon_{prog}$ = 1000%.

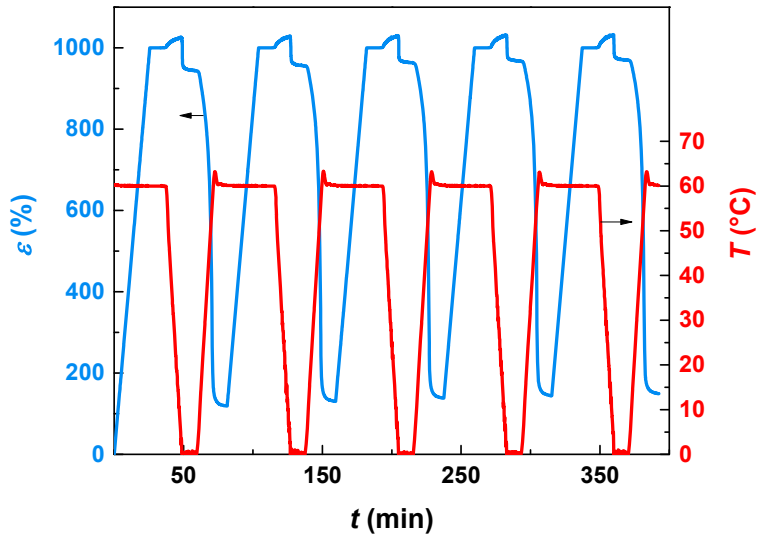


**Figure 2**. The macroscopic changes of the strain of **PCUU-10_5100** during 5 cycles of thermomechanical SME measurement ($\varepsilon_{prog}$ = 1000%).

The first cycle of the measurements was used to erase the thermal history of the samples as well as the effect of the amorphous chains flow, plastic deformation and relaxation,[32] and was not taken under consideration for the analysis of the shape-memory properties. The measurements were conducted with $\varepsilon_{prog}$ = 100-1000%. Firstly, the influence of $M_n$ of the soft segment, as well as of the hydrocarbon chain length between carbonate linkages on the shape-memory properties was investigated. When the samples of **PCUU-10** with different $M_n$ of the soft segment, stretched to $\varepsilon_{prog}$ = 100% were compared, it was noticed that with the increase of $M_n$ higher values of shape fixity ratios ($R_{f(2\text{-}5)}$) were achieved (Fig. 3a). This can be explained by the increasing degree of crystallinity with increasing length of the switching segment chain. Longer switching segment chains lead to higher flexibility and higher phase separation of the hard and switching domains, which in consequence increase the ability to crystallize within the switching segment domain. A similar increase of $R_{f(2\text{-}5)}$ was observed when the length of the α,ω-diol increased, for example in case of **PCUU-12_3500** when compared to **PCUU-10_3400**. Values of the average shape recovery ratio ($R_{r(2\text{-}5)}$) were slightly lower in case of samples with higher $M_n$ of the soft segment as well as with the length of the hydrocarbon chain between carbonate linkages. This can be attributed to the lower values of $\nu$, which means that the amount of netpoints determining the permanent shape within the hard domains was lower, and in consequence the possibility to recover the permanent shape decreased. The switching temperature ($T_{sw(2\text{-}5)}$), varying between 36 and 56 °C, strongly

correlated to the $T_m$ of the crystalline switching domains, and increased significantly with increasing hydrocarbon chain length in the switching segment repeating unit as well as with the switching segments' molecular weight. Remarkably, all the samples exhibited $R_{f(2-5)}$ > 93% and $R_{r(2-5)}$ > 98% after five cycles (Fig. 3a).

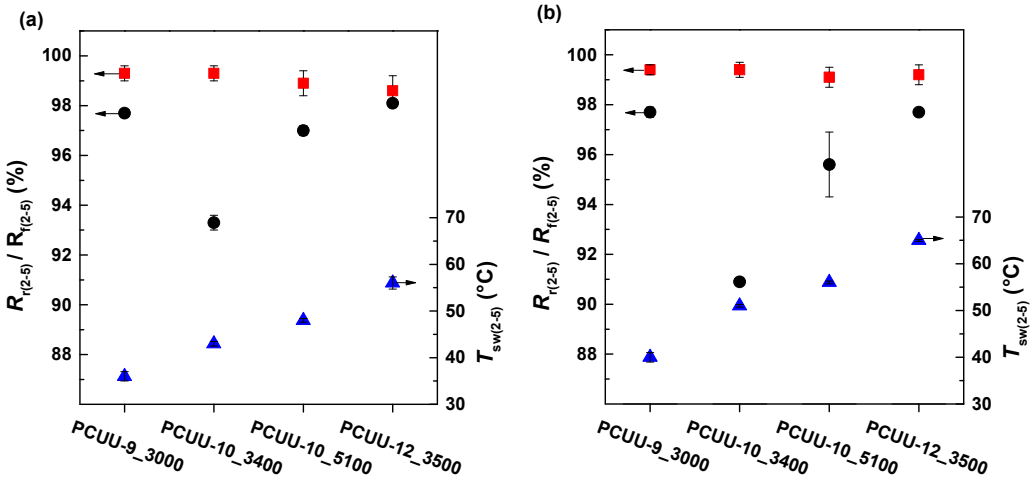


**Figure 3.** $R_{r(2-5)}$ (■), $R_{f(2-5)}$ (●) and $T_{sw(2-5)}$ (▲) values for PCUUs after 5 cycles in case of (a) $\varepsilon_{prog}$ = 100% and (b) $\varepsilon_{prog}$ = 600%.

In case of the sample **PCUU-9_3000** different relations between structure and shape-memory parameters were observed in comparison to samples based on 1,10-decanediol and 1,12-dodecanediol. Values of $R_{f(2-5)}$ and $R_{r(2-5)}$ of **PCUU-9_3000** were similar or higher in comparison to $R_{f(2-5)}$ and $R_{r(2-5)}$ of **PCUU-10_3400** and **PCUU-12_3500** (Table S1 in supplementary materials, Fig. 3a). Furthermore, this behavior of **PCUU-9_3000** became even more significant when $\varepsilon_{prog}$ was increased (exemplarily shown for $\varepsilon_{prog}$ = 600% in Fig. 3b). Properties of PCUUs based on oligocarbonate diols with odd and even number of methylene groups between the carbonate linkages strongly differs.[23] Structural investigations indicated that PCUU based on oligo(nonamethylene carbonate) diol contain more covalent cross-links and show the highest degree of phase separation among investigated samples (PCUU-9, PCUU-10, and PCUU-12).[23] Similarly, our results showed that **PCUU-9_3000** has the highest cross-linking density. The higher values of $R_{f(2-5)}$ and $R_{r(2-5)}$ of **PCUU-9_3000** in comparison to **PCUU-10_3400** and **PCUU-12_3500** can be explained by the higher amount of covalent crosslinks and the highest degree of phase separation.

With an increase of $\varepsilon_{prog}$, $R_{r(2-5)}$ slightly decreased, however the changes were very small. For example in case of **PCUU-12_3515**, $R_{r(2-5)}$ decreased from 98% to 97% when stretched to 100 and 1000%, respectively (Table S1, supplementary materials). No significant changes in values of $R_{r(2-5)}$ were observed with the change of $\varepsilon_{prog}$. When samples **PCUU-10_5100** and **PCUU-12_3515** were subjected to 4 cycles with 1000% deformation strain, they still maintained excellent shape-memory properties: $R_{f(2-5)} > 93\%$, $R_{r(2-5)} > 99\%$ and $R_{f(2-5)} > 97\%$, $R_{r(2-5)} > 99\%$, respectively. The influence of $\varepsilon_{prog}$ on the shape-memory properties is shown exemplarily for **PCUU-10_5100** in Figure 4.

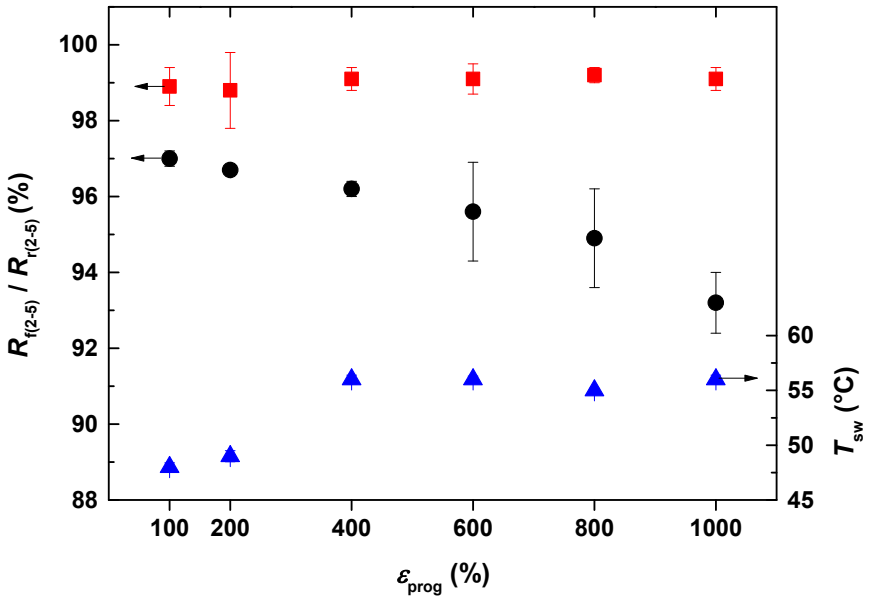


**Figure 4.** $R_{r(2-5)}$ (■), $R_{f(2-5)}$ (●) and $T_{sw(2-5)}$ (▲) values for **PCUU-10_5100** after 5 thermomechanical cycles with various $\varepsilon_{prog}$ (100-1000%).

The microstructural changes in the crystalline phase during the high-strain shape-memory measurements were studied by DSC and WAXS analyses. Samples were elongated to 100-1000% at $T_{prog} = 60$ °C in case of **PCUU-10_5100** or at $T_{prog} = 70$ °C in case of **PCUU-12_3500**, and held for 10 minutes under stress controlled conditions. Then sample was cooled to $T_{low} = 0$ or -10 °C, respectively, and the stress was reduced to $\sigma_0$, whereby the temporary shape was fixed. Stress was then completely removed and the sample was heated to RT. With the increase of $\varepsilon_{prog}$, a significant increase of the degree of crystallinity ($\chi_c$) followed by an increase of the $T_m$ and $\Delta H_m$ of the crystalline phase was observed (Tab. 5, Fig. 5 a). At the same time the crystal size ($l_c$) slightly

decreased with an increase of $\varepsilon_{prog}$, which can be attributed to an increase of lack of possible movement of the polymer chains with an increase of the elongation of the sample.

**Table 5.** Thermal and morphological properties of **PCUU-10_5100** and **PCUU-12_3500** with various $\varepsilon_{prog}$. *B* - Full width at half maximum of the crystalline reflection (in radians).

| Sample | $\varepsilon_{prog}$ (%) | $T_m$ (°C) | $\Delta H_m$ (J·g$^{-1}$) | $l_c$ (nm) | $\chi_c$ (%) | *B* |
|---|---|---|---|---|---|---|
| **PCUU-10_5100** | 0 | 42 ± 2 | 27 ± 1 | 12.8 ± 0.2 | 24.0 ± 2.2 | - |
| | 100 | 48 ± 2 | 45 ± 1 | 12.0 ± 0.2 | 26.5 ± 0.9 | 25.7 |
| | 200 | 49 ± 2 | 46 ± 1 | 12.2 ± 0.2 | 28.9 ± 1.1 | 22.5 |
| | 400 | 55 ± 2 | 50 ± 1 | 12.0 ± 0.2 | 31.3 ± 1.1 | 19.5 |
| | 600 | 57 ± 2 | 55 ± 1 | 11.5 ± 0.2 | 34.1 ± 1.2 | 19.6 |
| | 800 | 55 ± 2 | 55 ± 1 | 11.4 ± 0.2 | 36.7 ± 1.4 | 19.8 |
| | 1000 | 56 ± 2 | 54 ± 1 | 10.5 ± 0.2 | 38.1 ± 2.6 | 20.7 |
| **PCUU-12_3500** | 0 | 54 ± 2 | 39 ± 1 | 11.6 ± 0.2 | 22.2 ± 1.9 | - |
| | 100 | 53 ± 2 | 41 ± 1 | 10.4 ± 0.2 | 26.9 ± 0.4 | 27.4 |
| | 1000 | 63 ± 2 | 57 ± 1 | 10.1 ± 0.2 | 36.3 ± 1.7 | 21.0 |

Full width at half maximum of the crystalline reflection (in radians) (*B*) were measured to estimate the degree of sample orientation (Tab. 5). *B* decreased with increasing $\varepsilon_{prog}$, however, above $\varepsilon_{prog}$ = 400% no further orientation of the polymer chains was observed (Fig. 5 b). Constant degree of orientation is also visible in the WAXS patterns, in which the reflection area does not differ between 400 and 1000% (Fig. 6). Constant degree of orientation above 400% indicates that due to small amount of intermolecular covalent cross-links through the allophanate/biuret groups, further elongation only caused a chain shifting in the amorphous phase of the polymer, leading to new netpoints based on physical interactions (hydrogen bonds, crystallites in the soft segment domain).

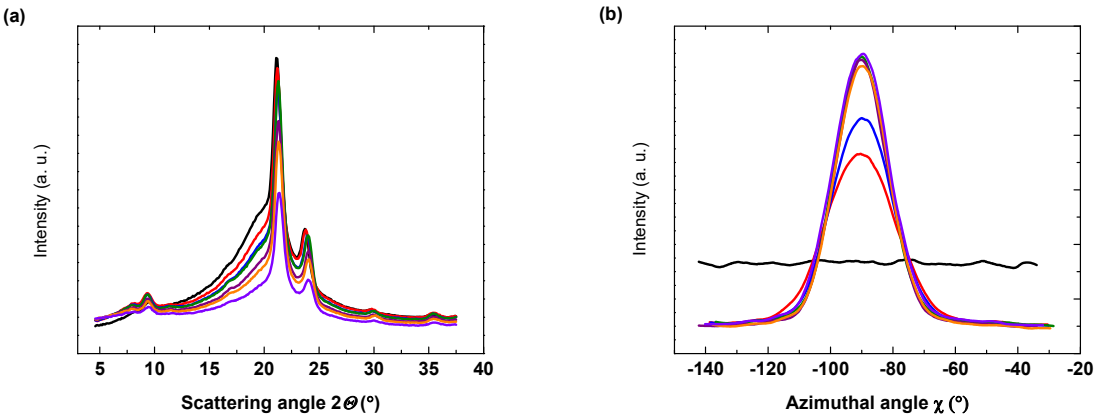


**Figure 5**. WAXS curves (a) and patterns of azimuthal angle χ (b) of **PCUU-10_5100** at RT after various $\varepsilon_{prog}$: 0% (▬), 100% (▬), 200% (▬), 400% (▬), 600% (▬), 800% (▬), and 1000% (▬).

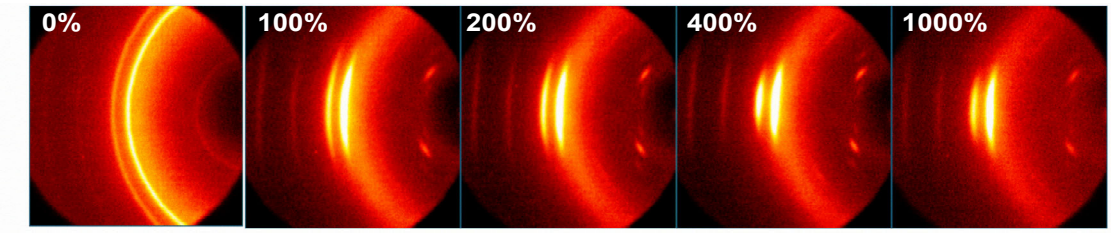


**Figure 6**. WAXS patterns of **PCUU-10_5100** at RT after various elongations: $\varepsilon_{prog}$ = 0, 100, 200, 400 and 1000%.

## 3. Conclusions

This work aimed at realizing high deformability with simultaneous high shape recovery ratio for shape-memory poly(carbonate-urea-urethane)s (PCUUs), which could be achieved by creating a polymer network providing two kinds of netpoints based on covalent bonds and physical interactions. Existence of a sufficient amount of inter-molecular bonds through the allophanate and biuret groups was essential to achieve shape-memory recovery ratio $R_r \geq 99\%$. Furthermore, highly crystallisable oligocarbonate diols provided a high shape fixity ratio ($R_f$ = 92-97%) of PCUUs. As a result, the investigated materials exhibited excellent high-strain shape-memory effect even when stretched to $\varepsilon_{prog}$ = 1000%, which is much higher deformation than reported so far. Moreover, the creation of new netpoints basing on physical interactions could be found by WAXS analysis when

the samples were elongated above 400% causing a crystallization of the polymer chains of the amorphous domains.

Poly(carbonate-urethane)s have been reported to have a good biostability and blood compatibility,[18] which together with the high-strain capacity and the shape-memory properties make obtained PCUUs interesting candidate materials for potential medical applications such as surgical sutures or vascular stents.

## Supporting Information

Additional supporting information can be found in the online version of this article at the publisher's website.

## Acknowledgments

Authors would like to thank Dr. Ulrich Nöchel for performing the WAXS analysis. This research has been supported by the European Union in the framework of European Social Fund through the Warsaw University of Technology Development Programme and within the project 34/ES/ZS-III/W-POKL/14 and partially through programme-oriented funding by the Helmholtz Association of German Research Centres.

## References

[1] B. Q. Y. Chan, S. S. Liow, X. J. Loh, *RSC Adv.* **2016**, *6*, 34946.
[2] Q. Zhao, H. J. Qi, T. Xie, *Prog. Polym. Sci.* **2015**, *49-50*, 79.
[3] S. Ainara, E. J. Foster, W. Christoph, E. Arantxa, C. Maria Angeles, *Smart Mater. Struct.* **2014**, *23*, 025033.
[4] A. Lendlein, R. Langer, *Science* **2002**, *296*, 1673.
[5] L. Sun, W. M. Huang, H. Lu, K. J. Lim, Y. Zhou, T. X. Wang, X. Y. Gao, *Macromol. Chem. Phys.* **2014**, *215*, 2430.
[6] W. Voit, T. Ware, R. R. Dasari, P. Smith, L. Danz, D. Simon, S. Barlow, S. R. Marder, K. Gall, *Adv. Funct. Mater.* **2010**, *20*, 162.
[7] F. Pilate, A. Toncheva, P. Dubois, J.-M. Raquez, *Eur. Polym. J.* **2016**, *80*, 268.
[8] T. Sauter, M. Heuchel, K. Kratz, A. Lendlein, *Polym. Rev.* **2013**, *53*, 6.
[9] K. K. Julich-Gruner, C. Löwenberg, A. T. Neffe, M. Behl, A. Lendlein, *Macromol. Chem. Phys.* **2013**, *214*, 527.
[10] Q. Zhao, M. Behl, A. Lendlein, *Soft Matter* **2013**, *9*, 1744.
[11] Y. Zhang, Q. Wang, C. Wang, T. Wang, *J. Mater. Chem.* **2011**, *21*, 9073.
[12] Y. Wang, X. Li, Y. Pan, Z. Zheng, X. Ding, Y. Peng, *RSC Adv.* **2014**, *4*, 17156.
[13] E. M. Christenson, S. Patel, J. M. Anderson, A. Hiltner, *Biomaterials* **2006**, *27*, 3920.

[14] M. Serkis, M. Špírková, R. Poręba, J. Hodan, J. Kredatusová, D. Kubies, *Polym. Deg. Stab.* **2015**, *119*, 23.
[15] H. J. Salacinski, M. Odlyha, G. Hamilton, A. M. Seifalian, *Biomaterials* **2002**, *23*, 2231.
[16] A. M. Seifalian, H. J. Salacinski, A. Tiwari, A. Edwards, S. Bowald, G. Hamilton, *Biomaterials* **2003**, *24*, 2549.
[17] L. Yang, J. Li, M. Li, Z. Gu, *Polymers* **2016**, *8*, 151.
[18] R. Zhu, Y. Wang, Z. Zhang, D. Ma, X. Wang, *Heliyon* **2016**, *2* e00125.
[19] J. Yang, Y. Gao, J. Li, M. Ding, F. Chen, H. Tan, Q. Fu, *RSC Adv.* **2013**, *3*, 8291.
[20] M. Shen, K. Zhang, P. Koettig, W. C. Welch, J. M. Dawson, *Eur. Spine J.* **2011**, *20*, 1837.
[21] S. L. Cooper, J. Guan, *Woodhead publishing series in biomaterials: Advances in polyurethane biomaterials*. Woodhead Publishing: 2016.
[22] D. K. Chattopadhyay, P. S. R. Prasad, B. Sreedhar, K. V. S. N. Raju, *Prog. Org. Coat.* **2005**, *54*, 296.
[23] M. M. Mazurek, K. Tomczyk, M. Auguścik, J. Ryszkowska, G. Rokicki, *Polym. Adv. Technol.* **2015**, *26*, 57.
[24] L. E. Alexander, *X-ray diffraction methods in polymer science*. Krieger: Huntington, N.Y., 1979.
[25] P. Scherrer, *Göttinger Nachrichten Math. Phys.* **1918**, *2*, 98.
[26] A. Lendlein, A. M. Schmidt, M. Schroeter, R. Langer, *J. Polym. Sci. A: Polym. Chem.* **2005**, *43*, 1369.
[27] C. Vasile, G. E. Zaikov, *Environmentally degradable materials based on multicomponent polymeric systems*. CRC Press: Leiden, 2009.
[28] K. Kratz, S. A. Madbouly, W. Wagermaier, A. Lendlein, *Adv. Mater.* **2011**, *23*, 4058.
[29] K. Kojio, M. Furukawa, S. Motokucho, M. Shimada, M. Sakai, *Macromolecules* **2009**, *42*, 8322.
[30] T. Masubuchi, M. Sakai, K. Kojio, M. Furukawa, T. Aoyagi, *e-J. Soft Mater.* **2007**, *3*, 55.
[31] J. Groll, M. Moeller, *Methods in enzymology, voulme 472*. Elsevier: 2010.
[32] Y. Feng, Y. Xue, J. Guo, L. Cheng, L. Jiao, Y. Zhang, J. Yue, *J. Appl. Polym. Sci.* **2009**, *112*, 473.
[33] F. Li, J. Hou, W. Zhu, X. Zhang, M. Xu, X. Luo, D. Ma, B. K. Kim, *J. Appl. Polym. Sci.* **1996**, *62*, 631.